

A Scalable, Incoherent-Light-Powered, Omnidirectional Self-Oscillator

Yasaman Nemati, Zixuan Deng, Haotian Pi, Hongshuang Guo, Hang Zhang, Arri Priimagi, and Hao Zeng*

Light-fueled self-oscillators based on stimuli-responsive soft materials have been explored toward the realization of a myriad of nonequilibrium robotic functions, such as adaptation, autonomous locomotion, and energy conversion. However, the high energy density and unidirectionality of the light field, together with the unscalable design of the existing demonstrations, hinder their further implementation. Herein, a light-responsive lampshade-like smart material assembly as a new self-oscillator model that is unfettered by the abovementioned challenges, is introduced. Liquid crystal elastomer with low phase transition temperature is used as the photomechanical component to provide twisting movement under low-intensity incoherent light field. A spiral lampshade frame ensures an equal amount of light being shadowed as negative feedback to sustain the oscillation upon constant light field from omnidirectional excitation (0° – 360° azimuth and 20° – 90° zenith). Different-sized oscillators with 6, 15, and 50 mm in diameter are fabricated to prove the possibility of scaling up and down the concept. The results provide a viewpoint on the fast-growing topic of self-oscillation in soft matter and new implications for self-sustained soft robots.

the Sun to fuel the materials' motion is a long-sought goal in functional materials research. Second, the optical fields allow for wireless powering and untethered operation. Third, the use of coherent light sources enables precisely controlled excitation and photoactuation with controllable degrees of freedom. Hence, light-controlled shape-morphing materials, such as liquid crystalline elastomers/polymers,^[10] photothermal bilayers,^[11] and hydrogels,^[12,13] are widely used in soft microrobotics,^[14–18] meeting many of the requirements of bio-inspired artificial systems^[19,20] and providing miniature tools for future medical treatment.^[21]

One emerging field of research in light-driven materials is light-fueled self-oscillating systems.^[22–25] A light-fueled self-oscillator is a responsive construct that can self-sustain its motion upon excitation by a constant optical field. By constant field, we mean stable light field without manual

1. Introduction


Photomechanical polymers are synthetic soft material systems that can undergo reversible shape changes in response to light illumination.^[1,2] Compared to other stimuli sources, e.g., chemicals,^[3] magnetic^[4] and electric fields,^[5] humidity,^[6] or heat,^[7–9] light possesses several advantages. First, light is a clean and omnipresent energy source, and harnessing the energy from

spatial/temporal modulation of light intensity. The key prerequisite for autonomous self-oscillation is to form a negative feedback loop between the light-induced material deformation and the energy absorption from the light field. This can be obtained through self-shadowing – a delicate design to attain self-regulation between the incident light beam and material movement.^[26,27] During the past decade, various reports on self-shadowing-induced oscillators in different polymer systems have been published,^[28–33] bringing about novel opportunities for soft microrobotics. Hitherto, self-sustained walkers,^[34] rollers,^[35] jumpers,^[36] swimmers,^[14,37] and water pumps^[38] have been demonstrated. The key technical aspect to attain those autonomous robotic systems relies on an unstable mechanical equilibrium, by which the input light energy induces a continuous mechanical vibration around the equilibrium point.^[39] The philosophy to drive responsive materials to their nonequilibrium states echoes the same principle rooted in the living systems, though in a highly simplified form.^[40]

Potential applications in material adaptation,^[41] autonomous locomotion,^[36] and energy conversion^[29,42] are preliminarily proposed for self-oscillators. Nevertheless, their further implementation is impeded by three major challenges. First, the light power used to fuel the self-sustained material motions is typically high, driven by a coherent laser beam with a small spot size and

Y. Nemati, Z. Deng, H. Guo, A. Priimagi, H. Zeng
Faculty of Engineering and Natural Sciences
Tampere University
P.O. Box 541, FI-33101 Tampere, Finland
E-mail: hao.zeng@tuni.fi

H. Pi, H. Zhang
Department of Applied Physics
Aalto University
P.O. Box 15100, FI 02150 Espoo, Finland

 The ORCID identification number(s) for the author(s) of this article can be found under <https://doi.org/10.1002/aisy.202300054>.

© 2023 The Authors. Advanced Intelligent Systems published by Wiley-VCH GmbH. This is an open access article under the terms of the Creative Commons Attribution License, which permits use, distribution and reproduction in any medium, provided the original work is properly cited.

DOI: 10.1002/aisy.202300054

high-energy dose focused on a specific spot on a material strip.^[14,37] This poses issues in simplification of the experimental setup arranged and the lifetime of the material used. Second, coherent, unidirectionally propagating laser beams facilitate the self-shadowing effect. Yet the potential application scenarios for self-oscillating materials would be greatly extended if the effect could be induced with incoherent light fields with uniform intensity over the entire structure—such as those obtained from, e.g., the Sun or flashlight. However, the existing self-oscillators fueled by incoherent light only function at certain incident angles,^[16,34,43] rendering them unsuitable for omnidirectional excitation. Third, most self-oscillators have been presented in the centimeter scale, and examples at both smaller and larger length scales are scarce.^[44–48] Demonstrations of scalability would be important for system generalization.^[49]

Here, we report a self-oscillating system that is unfettered by the abovementioned hurdles. The oscillator is assembled by a twisting soft actuating filament and a lampshade-like frame. The spiral-structured lampshade ensures an equal amount of light to excite/relax the filament actuator, which sets the foundation for the omnidirectional response. The filament actuator

made of liquid crystal elastomer (LCE) exhibits a remarkable response to low-intensity incoherent light field, e.g., the solar simulator. The concept of light-powered self-oscillating assembly is also demonstrated in up- and down-scaled dimensions.

2. Results

2.1. Highly Sensitive Light-Driven Material

Oscillation refers to periodic motion occurring upon repetitive material deformation at speed matching the oscillation frequency. Herein, we implement photothermally driven actuation due to its merits in deformation speed and reversibility compared to the photochemical one (occurring via photoisomerization of molecular constituents).^[50,51] To obtain a material system responding to low-intensity, incoherent light, eventually targeting actuation driven by direct sunlight, we choose an LCE with a low phase transition temperature ($\approx 40^\circ\text{C}$).^[52] The chemical structures of the constituent molecules are shown in **Figure 1a**. Thiol–Michael reaction is used to oligomerize diacrylate monomer (ST06512) and dithiol chain extender (EDDT),

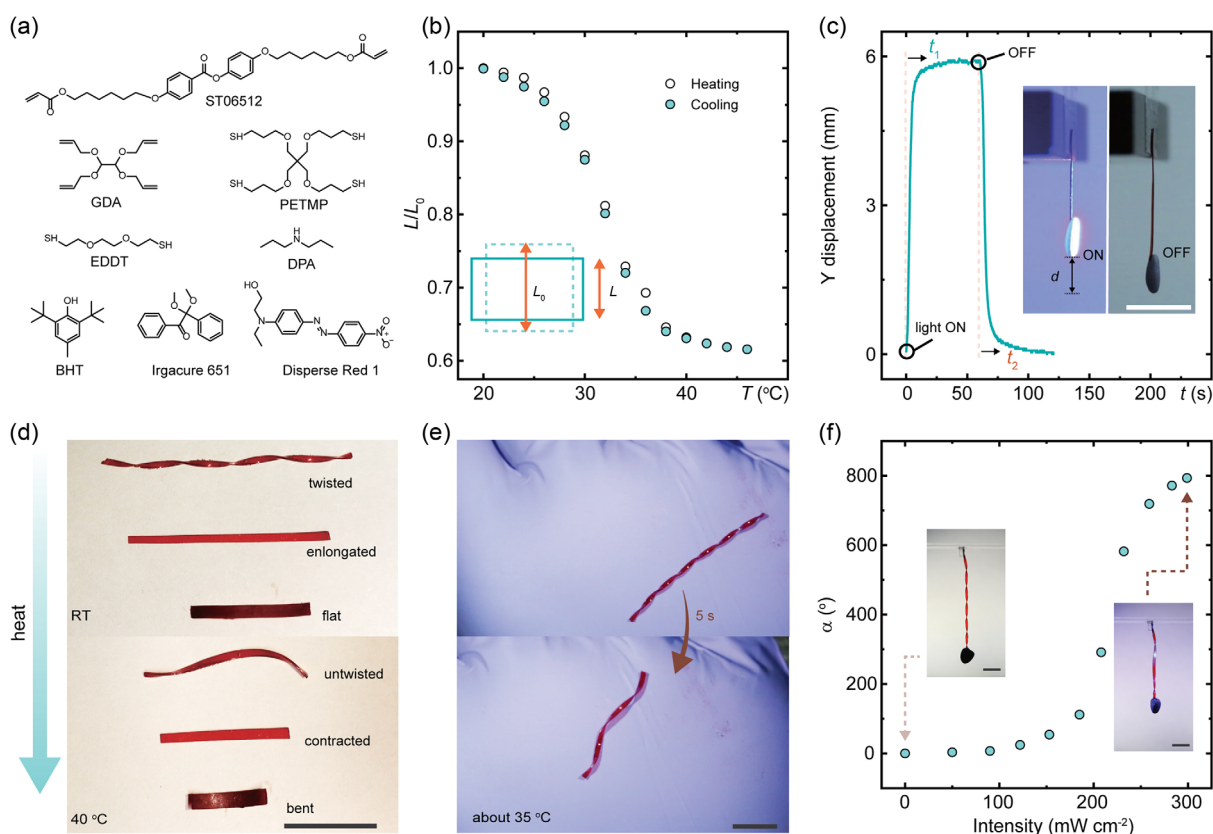


Figure 1. Highly sensitive light-responsive material. a) Compounds are used for fabricating the light-responsive LCE. b) Heat-induced deformation during one thermal cycle. Inset: schematic drawing of the deformation of a planar-aligned LCE. L_0 : original length along with the director. L : sample length after deformation. c) LCE contraction Y under light illumination. t_1 represents the duration from the pristine state to the maximal deformation state. t_2 represents the duration from the maximal deformation state to the pristine state after ceasing the light irradiation. Light: collimated LED source, 460 nm, 290 mW cm^{-2} . Sample dimensions: $15 \times 2 \times 0.25 \text{ mm}^3$. Insets: photographs of the LCE strip with (left) and without (right) light irradiation. d) Photographs of different LCE configurations at room temperature (top) and at 40°C (bottom). e) Photographs of a twisted LCE strip unwinding in response to human palm temperature. f) Untwisting angle versus light intensity. Insets: photographs of an unirradiated (left) and irradiated (460 nm, 300 mW cm^{-2}) LCE strip. Sample dimensions: $30 \times 2 \times 0.25 \text{ mm}^3$. All scale bars: 1 cm.

with the presence of a tetrafunctional thiol monomer (PETMP) and a catalyst dipropylamine (DPA) to form a loosely crosslinked prepolymer. The diacrylate monomer used contains only two aromatic rings, which has been reported to considerably reduce the actuation temperature.^[52] After the first polymerization, the elastic prepolymer is removed from the substrate and cut into strips. These strips are subjected to mechanical force to obtain a sequence of programmed alignment, which is then permanently fixed with UV radiation during the second polymerization to step-grow thiol-ene reaction with a tetrafunctional allyl ether monomer (GDA). Details of the sample preparation process are given in Figure S1a, Supporting Information and Experimental Section. Differential scanning calorimetry data are shown in Figure S2, Supporting Information.

Planar-aligned LCE (Figure S1b, Supporting Information) created by uniaxial stretching (200% compared to pristine length) exhibits thermo-driven contraction along the direction, as shown in Figure 1b. It undergoes a contraction strain of 30% at human skin temperature ($\approx 35^\circ\text{C}$) and reaches a maximal strain of $\approx 40\%$ at 46°C . Further details on the deformability along and perpendicular to the director and the mechanical properties of the LCE are given in Figure S3, Supporting Information. To endow the LCE light sensitive, Disperse Red 1 (DR1) is diffused into the LCE by immersing the strips into DR1-isopropanol solution (DR1:1-isopropanol = 1:100, wt%) at room temperature for 5 min. After diffusion, the LCE adapts a dark red color and undergoes macroscopic deformation in response to light illumination due to photothermal heating. Figure 1c shows the actuation kinetics upon light excitation. Details of the excitation time t_1 and relaxation time t_2 under different light intensities are given in Figure S4, Supporting Information.

Two-step crosslinking provides merit in arbitrarily programming the geometries and deformability through force-induced alignment inside the LCE network. Figure 1d shows examples of differently shaped samples and their corresponding deformations on a 40°C hot plate, i.e., twisting, contraction, and bending (see Experimental Section for sample preparation details). To demonstrate the high sensitivity of the material used, Figure 1e shows the LCE strip rapidly untwisting on a human palm (Movie S1, Supporting Information). Similar untwisting can be obtained upon light illumination, and the untwisting angle as a function of incident light intensity (460 nm) is given in Figure 1f. This sensitive light-induced twisting LCE forms the basis for the omnidirectional self-oscillator demonstration, as will be elaborated in the following section.

2.2. System Design for the Omnidirectional Light-Powered Self-Oscillator

To obtain an omnidirectional oscillator, we designed a plastic lampshade composed of four spiral segments and fabricated it using 3D printing. Details of the structural parameters are given in Figure S5, Supporting Information. A twisting LCE strip is fixed at the bottom center of the frame, while the entire structure is hanging vertically on a glass ceiling (Figure 2a). The spiral lampshade induces an equal amount of light shadowing from all illuminating angles (0° – 360° azimuth angle). Consequently, an identical length of LCE along the strip will be exposed to the light field to generate twisting movement that simultaneously causes the rotation of the outward lampshade. A negative feedback mechanism based on such self-shadowing is created, and it is independent of the incident angle, as schematically shown in

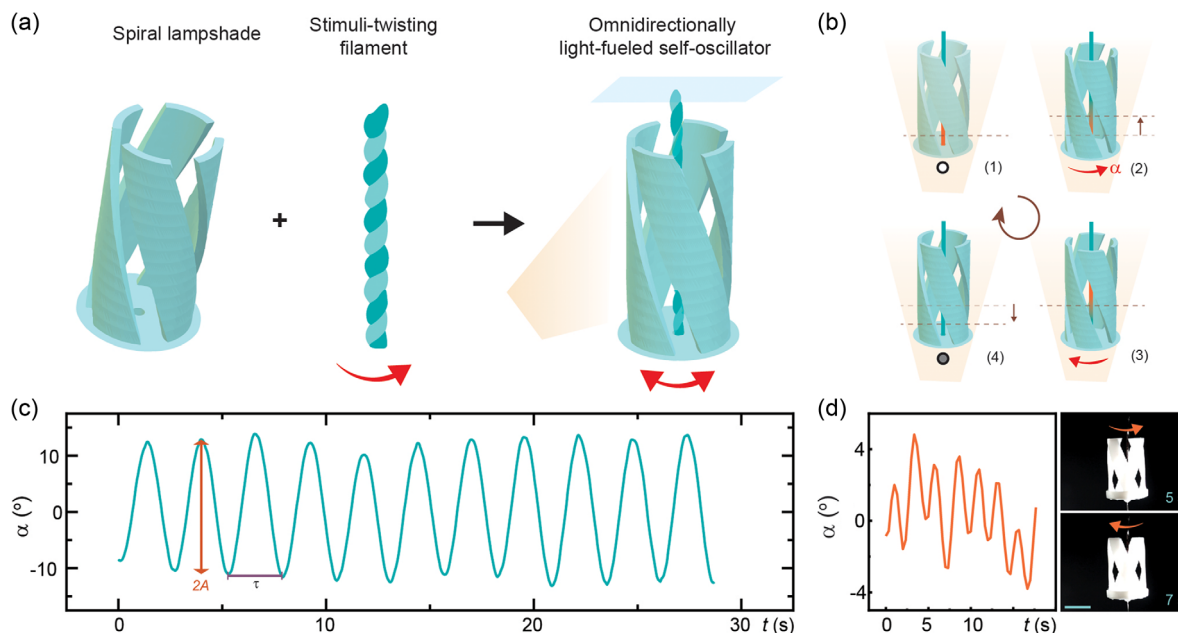


Figure 2. The optical design of omnidirectional self-oscillator. a) Schematic drawing of the assembly process. b) The self-shadowing mechanism for the self-oscillation through lampshade rotation. c) Twisting angle α versus t . Light: collimated LED source, 460 nm , 110 mW cm^{-2} . d) Sunlight-induced self-oscillation under a solar simulator. The twisting strip is painted with black ink from a permanent pen marker to enhance light absorption. Light: 100 mW cm^{-2} . Sample dimensions: $30 \times 1 \times 0.25\text{ mm}^3$. Scale bar: 1 cm .

Figure 2b. When the structure is exposed to light, one portion of the LCE, e.g., the bottom segment, as exemplified by step (1) in Figure 2b, twists due to photothermal heating. This causes the lampshade to twist by an angle α (step 2). The lampshade rotation changes the shadowing conditions, exposing the middle part of the LCE to light while the bottom segment gets blocked (step 3). The unilluminated bottom segment relaxes faster than the actuation of the middle part upon photothermal heating, yielding backward twisting and reverse rotation of the lampshade towards the original position (step 4). As a result, the relaxed bottom segment is again exposed to light, and a new oscillation cycle starts.

Upon illumination with incoherent light, i.e., a collimated LED beam, the lampshade structure self-oscillates with almost constant amplitude A and periodicity τ , as indicated in Figure 2c. The high light sensitivity also allows operation under direct sunlight. Figure 2d shows the data of a self-oscillator inside a simulated solar radiation environment in which one Sun intensity ($100 \pm 3 \text{ mW cm}^{-2}$) is illuminating the sample from a horizontal direction. The device self-oscillates but with a varying amplitude, which is due to the low intensity of the illuminating light. Details of sunlight-driven oscillation are depicted in Figure S6 and Movie S2, Supporting Information. Figure S7, Supporting Information, shows the spectra measurement of

the black ink-painted sample used for the simulated solar radiation.

2.3. Oscillation Under Omnidirectional Light Excitation

With the present configuration, the system can oscillate upon illumination at any azimuth angle, α_{az} . Due to the vertical arrangement, the decrease of zenith angle α_{zen} increases the incidence angle at the strip surface, which hence reduces the effective light intensity and light energy absorption. Thus, the oscillation behavior is α_{zen} -dependent. The geometrical relation between the device orientation, α_{az} , and α_{zen} is given in Figure 3a. Figure 3b shows the oscillation data as a function of light intensity at a fixed azimuth angle. More details on the intensity dependency can be found in Figure S8, Supporting Information. The oscillation amplitude A increases with intensity (Figure 3c) as more light energy is absorbed into the system to be dissipated as heat, causing enhanced mechanical movement. At the same time, the oscillation frequency increases from 0.36 to 0.51 Hz by increasing the intensity from 90 to 230 mW cm^{-2} . We ascribe the change in the oscillation period to the complicated nonlinearity in material responsiveness. Figure 3d shows the oscillation at a fixed zenith angle $\alpha_{\text{zen}} = 90^\circ$ but varying the α_{az} . Oscillation occurs over 0° – 360° illumination angle with bearable deviations

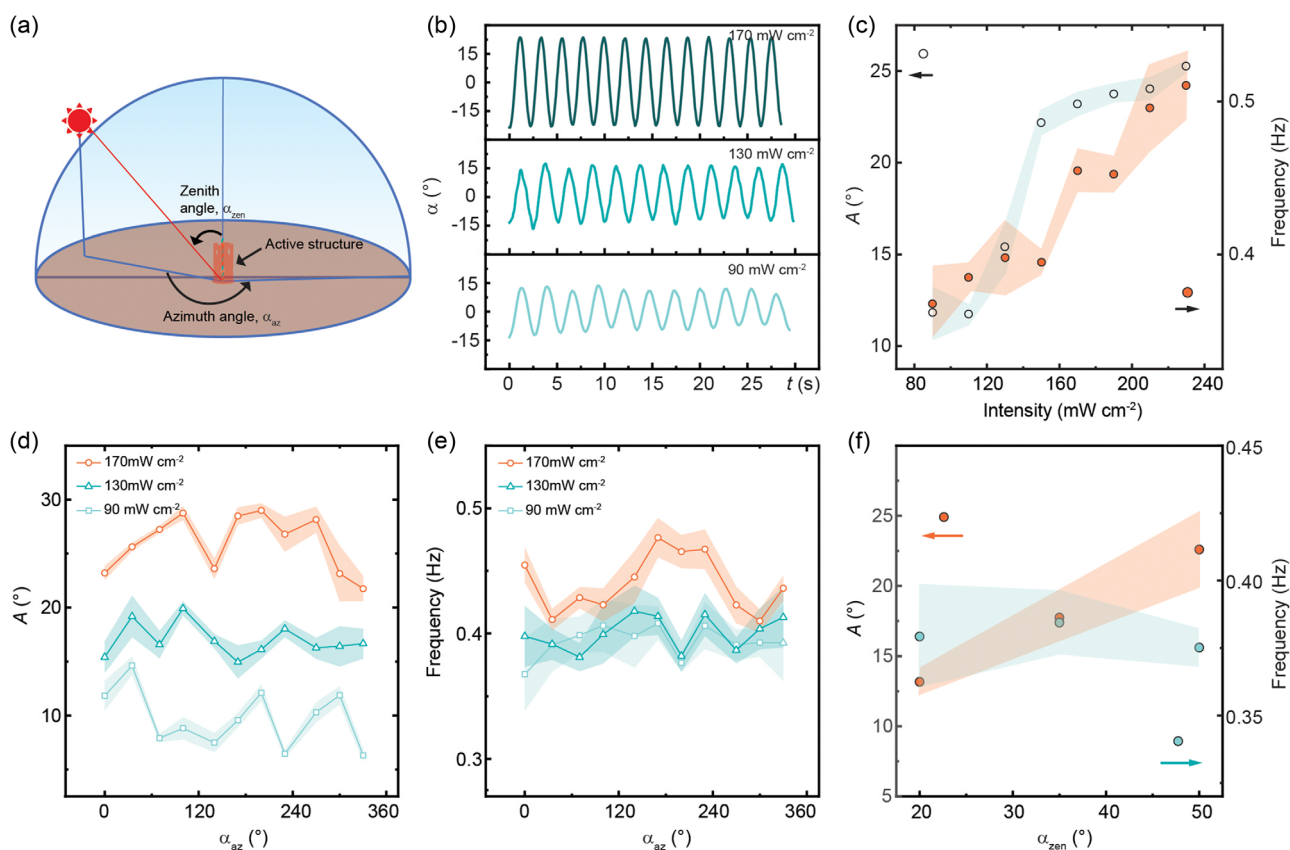


Figure 3. Oscillation under different incident angles. a) Schematic illustration for the definition of the azimuth and zenith angles. b) Time evolution of α at different intensities at $\alpha_{\text{az}} = 0^\circ$, $\alpha_{\text{zen}} = 90^\circ$. c) Amplitude (A) and frequency as a function of irradiation intensity. $\alpha_{\text{az}} = 0^\circ$, $\alpha_{\text{zen}} = 90^\circ$. Amplitude d) and frequency e) as a function of α_{az} upon excitation with different intensities at $\alpha_{\text{zen}} = 90^\circ$. f) Amplitude and frequency as a function of α_{zen} at $\alpha_{\text{az}} = 0^\circ$. Error bars indicate standard deviation for $n = 5$ measurements. Light: collimated LED source, 460 nm. Sample dimensions: $30 \times 1 \times 0.25 \text{ mm}^3$.

upon different intensities. Details of oscillation data at different α_{az} are given in Figure S9, Supporting Information. The change of A and frequency (Figure 3e) at different α_{az} is due to imperfections of the geometry, particularly the deviation of LCE strip from the central axis of the lampshade frame. At fixed azimuth angle $\alpha_{az} = 0^\circ$, similar frequencies are recorded upon change of α_{zen} , while A increases with α_{zen} (Figure 3f) as the effective light intensity is increased. More details on α_{zen} -dependent oscillation are given in Figure S10, Supporting Information.

Achieving similar self-oscillation behavior independent from the excitation direction requires an equal amount of material actuation on the central filament. This can be obtained by using a spiral design of the lampshade (with both handedness) to enable the same amount of light shadow area projected onto the actuator from the light beam excited from any azimuthal angle. Hence, this omnidirectional self-oscillation concept can also be applied to other lampshade designs to create the negative feedback loop, as exemplified by a spiral lampshade and corresponding self-oscillation data shown in Figure S11, Supporting Information.

2.4. Up- and Down-Scaling

The lampshade design brings the opportunity to scale the system concept up and down in size. As the lampshade frame can be fabricated through 3D printing or paper cutting, the key is to find a suitable twisting actuator to mechanically support the hung structure, meanwhile providing sufficient twisting photoactuation for rotating the lampshade. **Figure 4a** shows lampshades with 6, 15, and 50 mm diameters. For the central filament

actuator, a twisting LCE strip is used for 6 and 15 mm-sized oscillators with 0.24 and 0.76 mg mass, respectively, while the 50 mm-sized one is integrated with a thermo-sensitive metallic spring (4.7 g). The metallic spring is taken from a household thermometer, which provides 30° rotation per 10°C temperature elevation. Details on the metallic spring preparation and its light-induced twisting angle characterization are given in Figure S12 and S13, Supporting Information. All the different-sized lampshades can self-oscillate under constant light irradiation from a collimated LED source, as shown in Figure 4c. The 6 mm-sized oscillator exhibits a higher oscillating frequency (0.72 Hz) compared to the 15 mm-sized one (0.52 Hz). This is due to the elevation of resonance frequency in the down-scaled structure. It is worth noting that the frequency of the up-scaled oscillator should not be compared with the other two since the high stiffness of the metallic spring enhances the resonance frequency of the structure. Details of oscillation in the large-sized oscillator are given in Figure S14 and Movie S3, Supporting Information.

3. Discussion and Conclusion

Living systems are not closed, as energy and/or materials transfer with their environment (both in influx and dissipation perspectives) are constantly taking place. Therefore, they are no longer considered as being at a thermodynamic equilibrium state but operating far from equilibrium.^[53] To adapt to the environment and self-regulate their action in response to it, living entities have exploited efficient approaches to address this process by functioning around instabilities that are maintained in a

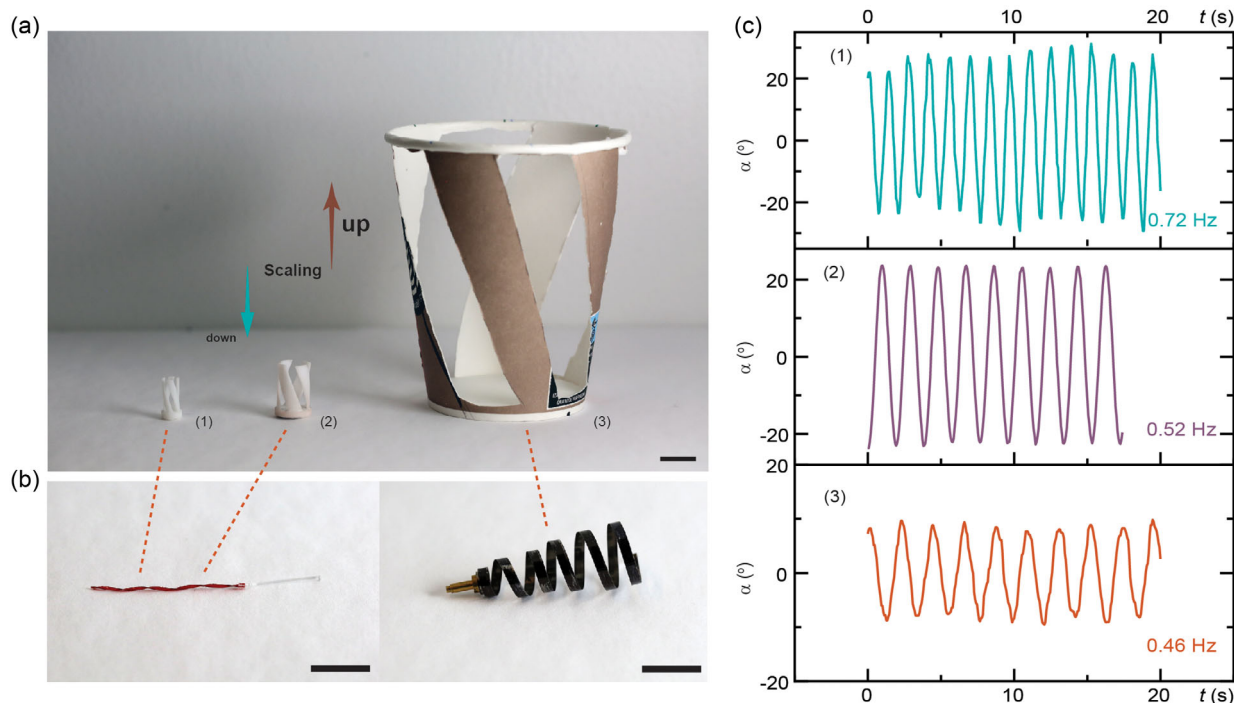


Figure 4. Scalable light-powered self-oscillator. a) Photograph of lampshade structures in different sizes. b) Photographs of responsive filaments used in the self-oscillator structure. All scale bars: 1 cm. c) Light-powered self-oscillation for 1) 6 mm, 2) 15 mm, and 3) 50 mm sized structures. Light: collimated LED source, 460 nm , 190 cm^{-2} for (1), 230 mW cm^{-2} for (2), 170 mW cm^{-2} for (3).

controllable manner.^[54] Taking the well-known Venus flytrap as an example, the fast closure of the trap results from the snap-buckling instability, where a small perturbation can trigger the onset of the instability and push the system transiently from one unstable state toward the other one.^[55] Counterintuitively, the leaf is not operating in its global energy minimum state but in an intermediate unstable state, which enables the occurrence of rapid closure. This case demonstrates that by building the system around instability thresholds, fast and effective actions are enabled, as small energy inflow is needed to cross the energy barriers.

Self-oscillation is a mechanically nonequilibrium material state that results in continuous motion under constant field excitation. This state provides an avenue to achieve robotic motion without the need for explicit human control and to introduce new functionality for structures to self-adapt to their environment. In this study, we investigate the behavior of an oscillating lampshade as an example of nonequilibrium soft matter. Our results, together with other recent examples in the field,^[19,56,57] point to a new path for the development of life-like systems.

We report a light-powered lampshade oscillator that can autonomously self-oscillate upon a constant light field without human manipulation. LCE with low phase transition temperature provides high light sensitivity in twisting and efficient rotation in photomechanical actuation. The twisting motion used distinguishes this study from most self-oscillators realized up to date, which are predominantly based on bending or contracting deformation modes. The lampshade frame composed of four spiral segments ensures light shadowing from omnidirectional incident angles and yields an effective negative feedback loop to sustain the oscillation. Self-oscillation data are recorded over 0°–360° azimuth and 20°–90° zenith angle, with reasonable deviation in oscillation amplitude and frequency due to the imperfection of the structural geometry. We have fabricated oscillators with 6, 15, and 50 mm in diameter to prove the principle of up-scaling and down-scaling. The up-scaling omnidirectional self-oscillator also demonstrates the possibility of devising autonomous actuators from household materials. The results provide a new alternative for self-sustained materials and soft robots, driven by low-power irradiation.

4. Experimental Section

Materials in Brief: ST06512 (4-(6-(acryloyloxy)hexyloxy)phenyl 4-(6-(acryloyloxy)hexyloxy)benzoates) was obtained from SYNTHON Chemicals. GDA (tetraallyloxyethane) and DPA were obtained from TCI. EDDT (2,2'-(ethylenedioxy)diethanethiol), PETMP (pentaerythritol tetraakis(3-mercaptopropionate)), BHT (2,6-di-*tert*-butyl-4-methylphenol), Irgacure 651 (2,2-dimethoxy-2-phenylacetophenone), and DR1 were obtained from Sigma-Aldrich. All chemicals were used as received.

LCE Fabrication: Liquid crystal cells were prepared by gluing two coated glass slides (polyvinyl alcohol, 5 wt% water solution, 4000 RPM, 1 min, baked at 100 °C for 10 min), separated by 250 μm spacers. The liquid crystal mixture was prepared by firstly melting 0.27 mmol ST06512, 1 wt% BHT, and 1.5 wt% of Irgacure 651 in a vial at 80 °C. The melted mixture was then cooled down to room temperature before adding 0.27 mmol EDDT, 0.015 mmol PETMP, 0.03 mmol GDA, and 0.5 wt% DPA. The mixture was manually stirred and then filled into a 250 μm thick cell via capillary force at 80 °C. The cell was kept in an oven at 80 °C for 24 h to allow for the thiol-Michael reaction to occur. Then the cell was opened by a blade, and strips were cut from the film. The strips were subjected to varied mechanical forces to obtain different configurations, followed by UV

polymerization (365 nm, 180 mW cm⁻², 5 min). Finally, the polymerized strips were immersed in DR1-isopropanol solution (DR1:1-isopropanol = 1:100, wt%) at room temperature for 5 min before ready to use.

Oscillator Fabrication: The oscillator was made up of two parts: the spiral lampshade and the twisting filament. For the 6 and 15 mm-sized oscillators, the lampshade design was modeled in SOLIDWORKS (2021), and the structures were fabricated using a Form2 3D printer (Formlabs Inc.). For the 50 mm-sized oscillator, a thermometer spring was utilized as the twisting filament, and the lampshade design was fabricated by cutting the spiral geometry on a paper coffee cup. In all oscillators, a small mass was added to the bottom of the lampshade to lower the mass center and ensure that the structure remained vertical.

Optical Characterization: Photographs and movies of omnidirectional self-oscillation were captured with Canon 5D Mark III camera with 100 mm lens. An LED source (CoolLED pE-4000) was used for light excitation. A rotating stage was used to manually change the strip facet for azimuthal angle-dependent measurements. A solar simulator (OAI TriSol 7 kW CPV-simulator) was used for the sunlight-powered oscillation measurements.

Data Analysis: The quantitative data were extracted from the recorded movie with video analysis software (Tracker).

Supporting Information

Supporting Information is available from the Wiley Online Library or from the author.

Acknowledgements

Y.N. and Z.D. contributed equally to this work. The authors acknowledge funding from the Academy of Finland (Postdoctoral Researcher No. 331015 to H. Zhang, Research Fellow No. 340263 to H. Zeng, Center of Excellence in Life-Inspired Hybrid Materials—LIBER No. 346107 and the Flagship Programme on Photonics Research and Innovation, PREIN, No. 320165 to A.P.). Y.N. and Z.D. are supported by European Union's Horizon 2020 Research and Innovation Programme under the Marie Skłodowska-Curie Grant Agreement 956150 (STORM-BOTS), No. 31221956150. H. Zeng gratefully acknowledges the financial support of the European Research Council (Starting Grant project ONLINE, No. 101076207). The authors thank Murthy Grandhi and Paola Vivo for instructing with the use of the solar simulator.

Conflict of Interest

The authors declare no conflict of interest.

Data Availability Statement

The data that support the findings of this study are available from the corresponding author upon reasonable request.

Keywords

liquid crystal elastomer, micro-robot, photoactuator, self-oscillator, self-sustained motion

Received: January 30, 2023

Revised: March 15, 2023

Published online:

- [1] M. Pilz da Cunha, M. G. Debije, A. P. H. J. Schenning, *Chem. Soc. Rev.* **2020**, *49*, 6568.
- [2] J. M. McCracken, B. R. Donovan, T. J. White, *Adv. Mater.* **2020**, *32*, 1906564.
- [3] M. Hua, C. Kim, Y. Du, D. Wu, R. Bai, X. He, *Matter* **2021**, *4*, 1029.
- [4] W. Hu, G. Z. Lum, M. Mastrangeli, M. Sitti, *Nature* **2018**, *554*, 81.
- [5] Z. Yoder, D. Macari, G. Kleinwaks, I. Schmidt, E. Acome, C. Keplinger, *Adv. Funct. Mater.* **2023**, *33*, 2209080.
- [6] B. Shin, J. Ha, M. Lee, K. Park, G. H. Park, T. H. Choi, K.-J. Cho, H.-Y. Kim, *Sci. Robot.* **2018**, *3*, eaar2629.
- [7] Y. Zhang, Z. Wang, Y. Yang, Q. Chen, X. Qian, Y. Wu, H. Liang, Y. Xu, Y. Wei, Y. Ji, *Sci. Adv.* **2020**, *6*, eaay8606.
- [8] K. Li, C. Du, Q. He, S. Cai, *Extreme Mech. Lett.* **2022**, *50*, 101547.
- [9] A. S. Kuentler, Y. Chen, P. Bui, H. Kim, A. DeSimone, L. Jin, R. C. Hayward, *Adv. Mater.* **2020**, *32*, 2000609.
- [10] Y.-Y. Xiao, Z.-C. Jiang, Y. Zhao, *Syst.* **2020**, *2*, 2000148.
- [11] S. Wang, Y. Gao, A. Wei, P. Xiao, Y. Liang, W. Lu, C. Chen, C. Zhang, G. Yang, H. Yao, T. Chen, *Nat. Commun.* **2020**, *11*, 4359.
- [12] H. Kim, J.-H. Kang, Y. Zhou, A. S. Kuentler, Y. Kim, C. Chen, T. Emrick, R. C. Hayward, *Adv. Mater.* **2019**, *31*, 1900932.
- [13] A. Mourran, H. Zhang, R. Vinokur, M. Möller, *Adv. Mater.* **2017**, *29*, 1604825.
- [14] Y. Zhao, C. Xuan, X. Qian, Y. Alsaïd, M. Hua, L. Jin, X. He, *Sci. Robot.* **2019**, *4*, eaax7112.
- [15] C. Li, G. C. Lau, H. Yuan, A. Aggarwal, V. L. Dominguez, S. Liu, H. Sai, L. C. Palmer, N. A. Sather, T. J. Pearson, D. E. Freedman, P. K. Amiri, M. O. de la Cruz, S. I. Stupp, *Robot.* **2020**, *5*, eabb9822.
- [16] A. H. Gelebart, D. Jan Mulder, M. Varga, A. Konya, G. Vantomme, E. W. Meijer, R. L. B. Selinger, D. J. Broer, *Nature* **2017**, *546*, 632.
- [17] J. Yang, H. Zhang, A. Berdin, W. Hu, H. Zeng, *Adv. Sci.* **2022**, *10*, 2206752.
- [18] J. Jeon, J.-C. Choi, H. Lee, W. Cho, K. Lee, J. G. Kim, J.-W. Lee, K.-I. Joo, M. Cho, H.-R. Kim, J. J. Wie, *Mater. Today* **2021**, *49*, 97.
- [19] H. Zhang, H. Zeng, A. Eklund, H. Guo, A. Priimagi, O. Ikkala, *Nat. Nanotechnol.* **2022**, *17*, 1303.
- [20] S. Li, M. M. Lerch, J. T. Waters, B. Deng, R. S. Martens, Y. Yao, D. Y. Kim, K. Bertoldi, A. Grinthal, A. C. Balazs, J. Aizenberg, *Nature* **2022**, *605*, 76.
- [21] J.-a. Lv, Y. Liu, J. Wei, E. Chen, L. Qin, Y. Yu, *Nature* **2016**, *537*, 179.
- [22] H. Zeng, M. Lahikainen, L. Liu, Z. Ahmed, O. M. Wani, M. Wang, H. Yang, A. Priimagi, *Nat. Commun.* **2019**, *10*, 5057.
- [23] G. Vantomme, L. C. M. Elands, A. H. Gelebart, E. W. Meijer, A. Y. Pogromsky, H. Nijmeijer, D. J. Broer, *Nat. Mater.* **2021**, *20*, 1702.
- [24] K. Obara, Y. Kageyama, S. Takeda, *Small* **2022**, *18*, 2105302.
- [25] Y. Li, Y. Liu, D. Luo, *Adv. Opt. Mater.* **2021**, *9*, 2001861.
- [26] T. J. White, N. V. Tabiryan, S. V. Serak, U. A. Hrozhyk, V. P. Tondiglia, H. Koerner, R. A. Vaia, T. J. Bunning, *Soft Matter* **2008**, *4*, 1796.
- [27] A. H. Gelebart, G. Vantomme, E. W. Meijer, D. J. Broer, *Adv. Mater.* **2017**, *29*, 1606712.
- [28] Z. Hu, Y. Li, J.-a. Lv, *Nat. Commun.* **2021**, *12*, 3211.
- [29] J. Wang, B. Yang, M. Yu, H. Yu, *ACS Appl. Mater. Interfaces* **2022**, *14*, 15632.
- [30] F. Ge, R. Yang, X. Tong, F. Camerel, Y. Zhao, *Angew. Chem. Int. Ed.* **2018**, *57*, 11758.
- [31] Z.-Z. Nie, B. Zuo, M. Wang, S. Huang, X.-M. Chen, Z.-Y. Liu, H. Yang, *Nat. Commun.* **2021**, *12*, 2334.
- [32] W. Wei, Z. Zhang, J. Wei, X. Li, J. Guo, *Adv. Opt. Mater.* **2018**, *6*, 1800131.
- [33] X. Dong, J. Xu, X. Xu, S. Dai, X. Zhou, C. Ma, G. Cheng, N. Yuan, J. Ding, *ACS Appl. Mater. Interfaces* **2020**, *12*, 6460.
- [34] Y. Hu, Q. Ji, M. Huang, L. Chang, C. Zhang, G. Wu, B. Zi, N. Bao, W. Chen, Y. Wu, *Angew. Chem. Int. Ed.* **2021**, *60*, 20511.
- [35] X. Lu, S. Guo, X. Tong, H. Xia, Y. Zhao, *Adv. Mater.* **2017**, *29*, 1606467.
- [36] Y. Zhao, Y. Hong, F. Qi, Y. Chi, H. Su, J. Yin, *Adv. Mater.* **2023**, *35*, 2207372.
- [37] Z. Li, N. V. Myung, Y. Yin, *Sci. Robot.* **2021**, *6*, eabi4523.
- [38] Z. Deng, H. Zhang, A. Priimagi, H. Zeng, *Adv. Mater.* **2023**, 2209683.
- [39] T. Sun, K. Li, Y. Dai, J. Zhao, *Int. J. Mech. Sci.* **2022**, *227*, 107439.
- [40] M. M. Lerch, A. Grinthal, J. Aizenberg, *Adv. Mater.* **2020**, *32*, 1905554.
- [41] F. Zhai, Y. Feng, Z. Li, Y. Xie, J. Ge, H. Wang, W. Qiu, W. Feng, *Matter* **2021**, *4*, 3313.
- [42] L. Chang, D. Wang, Z. Huang, C. Wang, J. Torop, B. Li, Y. Wang, Y. Hu, A. Aabloo, *Adv. Funct. Mater.* **2022**, 2212341.
- [43] J. Sun, W. Hu, L. Zhang, R. Lan, H. Yang, D.-K. Yang, *Adv. Funct. Mater.* **2021**, *31*, 2103311.
- [44] T. Ikegami, Y. Kageyama, K. Obara, S. Takeda, *Angew. Chem. Int. Ed.* **2016**, *55*, 8239.
- [45] F. Tong, D. Kitagawa, I. Bushnak, R. O. Al-Kaysi, C. J. Bardeen, *Angew. Chem. Int. Ed.* **2021**, *60*, 2414.
- [46] A. Baumann, A. Sánchez-Ferrer, L. Jacomine, P. Martinoty, V. Le Houerou, F. Ziebert, I. M. Kulić, *Nat. Mater.* **2018**, *17*, 523.
- [47] Y. Zhai, T. N. Ng, *Adv. Intell. Syst.* **2021**, 2100085.
- [48] A. K. Bartholomew, I. B. Stone, M. L. Steigerwald, T. H. Lambert, X. Roy, *J. Am. Chem. Soc.* **2022**, *144*, 16773.
- [49] X. Chen, D. Goodnight, Z. Gao, A. H. Cavusoglu, N. Sabharwal, M. DeLay, A. Driks, O. Sahin, *Nat. Commun.* **2015**, *6*, 7346.
- [50] M. Yamada, M. Kondo, J.-I. Mamiya, Y. Yu, M. Kinoshita, C. J. Barrett, T. Ikeda, *Angew. Chem. Int. Ed.* **2008**, *47*, 4986.
- [51] S. Nocentini, D. Martella, C. Parmeggiani, S. Zanotto, D. S. Wiersma, *Adv. Opt. Mater.* **2018**, *6*, 1800167.
- [52] G. E. Bauman, J. M. McCracken, T. J. White, *Angew. Chem. Int. Ed.* **2022**, *61*, e202202577.
- [53] J. L. England, *Nat. Nanotechnol.* **2015**, *10*, 919.
- [54] P. Fratzl, W. Schäffner, in *Active Materials* (Eds: F. Peter, F. Michael, K. Karim, S. Wolfgang), De Gruyter, Berlin **2022**, p. 37.
- [55] Y. Forterre, J. M. Skotheim, J. Dumais, L. Mahadevan, *Nature* **2005**, *433*, 421.
- [56] J. G. Kim, J. Jeon, R. Sivakumar, J. Lee, Y. H. Kim, M. Cho, J. H. Youk, J. J. Wie, *Syst.* **2022**, *4*, 2100148.
- [57] X. Yang, W. Shi, Z. Chen, M. Du, S. Xiao, S. Qu, C. Li, *Adv. Funct. Mater.* **2023**, 2214394.